errors in nominal or initial conditions. The use of a single reference trajectory in each problem means that the guidance method requires little storage capacity.

In the lunar landing study, the guidance capability for a control system formulated with the gravity turn as the reference trajectory was far superior to one formulated with a constant-pitch-rate reference trajectory. With a single gravity turn reference trajectory, the guidance system could compensate for initial range errors of 100% of the reference value with a small additional fuel increment, equivalent to a characteristic velocity of 70 fps.

In the earth re-entry problem it was found that with a single reference trajectory it was possible to obtain a guidance capability from 1500 to 12,000 miles for a range of entry conditions which utilized virtually all of the vehicle's capability.

For the abort conditions considered in this paper, the guidance system was generally able to make almost full use of the vehicle's range capability.

Errors of 5% in vehicle L/D had little effect on the capability of this guidance scheme.

Density variations from the nominal affected the long-range guidance but had little effect on guidance capability for ranges less than 6000 miles.

References

[1] McLean, J. D., Schmidt, S. F., and McGee, L. A., "Optimal filtering and linear prediction applied to a midcourse navigation system for the circumlunar mission," NASA TN D-1208 (1962).

[2] Wingrove, R. C. and Coate, R. E., "Lift control during atmosphere entry from supercircular velocity," *Proceedings of the IAS-NASA National Meeting on Manned Space Flight* (Institute Aerospace Sciences, New York, 1962), pp. 95–105.

[3] Morth, R. and Speyer, J., "Control system for supercircular entry maneuvers," Inst. Aerospace Sci. Paper 62-3 (January 1962).

[4] Foudriat, E. C., "Study of the use of a terminal controller technique for re-entry guidance of a capsule-type vehicle," NASA TN D-828 (1961).

[5] Bryson, A. E. and Denham, W. F., "A guidance scheme for supercircular re-entry of a lifting vehicle," ARS Preprint 2299-61 (October 1961).

[6] Bliss, G. A., *Mathematics for Exterior Ballistics* (John Wiley and Sons, Inc., New York, 1944), pp. 63–96.

[7] Tsien, H. S., *Engineering Cybernetics* (McGraw-Hill Book Co., Inc., 1954), pp. 178–197.

[8] Faget, M. A. and Mathews, C. W., "Manned lunar landing," Aerospace Eng. 21, 50–52 (January 1962).

[9] Citron, S. J., Dunin, S. E., and Meissinger, H. F., "A self-contained terminal guidance technique for lunar landing," ARS Preprint 2685-62 (November 1962).

MARCH-APRIL 1964 J. SPACECRAFT VOL. 1, NO. 2

Quadrupedal Landing Gear Systems for Spacecraft

RAYMOND J. BLACK*

The Bendix Corporation, South Bend, Ind.

Landing gear systems having multiple legs, each of which is an inverted tripod composed of three energy-absorbing struts, are studied. Model scaling is related to three primary full-scale to model ratios: acceleration, mass, and length. Model drop test results correlate satisfactorily with theoretical landing stability ($\dot{y}$ vs $\dot{x}$) curves for models simulating 1) a 70-ft-high, 2000-slug vehicle and 2) an 18-ft-high, 300-slug vehicle. A squat, "wide track" system for ground slopes up to 15° is also studied. The theoretical model and the results of a parametric study are given in terms of ground slope (5°, 7°, and 15°), tripodal strut stroke loads, lower/upper strut load ratio, and number of legs. A 4-leg system is shown to be best; a 5-leg system would be approximately 25% heavier because, in the critical-stroke landing condition (uphill impact), ¾ of the total vehicle kinetic energy had to be absorbed by the one leg making first contact for either system. The critical stability landing is a downhill, back-pitched, 2-2 impact. Landing gear weight must be doubled to increase ground-slope capability from 5°–7° to 15°.

Nomenclature

b_{ij} = angle, as seen in side view of vehicle, made by jth shock strut of ith leg set (Fig. 5)

c_{ij} = angle, as seen in true view of jth shock strut of ith leg set (Fig. 5)

d_{0j} = vertical distance from hardpoint of no. 1 strut to hardpoint of jth strut (Fig. 5)

d_1 = vertical distance from vehicle center of gravity to hardpoint of no. 1 strut (Fig. 5)

d_{i1} = distance, in Z direction, from hardpoint of no. 1 strut to pad connection point (Fig. 5)

F_c = total effective vertical load output of one leg set

F_{ij} = axial force of jth shock strut of ith leg set (Fig. 7)

F_j = plastic stroking force of jth shock strut (Fig. 7)

F_{ia},F_{ib},F_{ic} = set of triaxial forces acting on ith pad (vehicle axes) (Fig. 6)

F_{iz} = vertical force on pad

g = acceleration of gravity (local)

h_1 = rise of lower link of drop test mechanism (Fig. 3)

h_2 = drop height of dynamic model (Fig. 3)

I = moment of inertia of vehicle about pitch axis

I_0 = moment of inertia of lower link of drop test mechanism

K_j = compression spring rate of jth energy absorber (Fig. 7)

K_{Ej} = extensional spring rate of jth shock strut

K_s = vertical spring rate of vehicle and pad (per leg set) (Fig. 6)

L = instantaneous center of rotation of lower link of drop test mechanism (Fig. 3)

L_p = crushable thickness of landing pad

L_{ij} = length of jth shock strut of ith leg set as seen in

Received August 23, 1963; revision received December 23, 1963.

* Developmental Engineer, Advanced Mechanics Department, Bendix Products Aerospace Division.

side view of vehicle (Fig. 5)
L_{ijt} = true length of jth shock strut of ith leg set (Fig. 5)
L_{ijt0} = initial true length of jth shock strut of ith leg set
m = mass of vehicle
m_0 = mass of lower link of drop test mechanism
m_p = unsprung mass of a leg set
n = number of legs
P_j = hysteresis force in jth shock strut energy absorber (Fig. 7)
$\dot{s}_i$ = absolute sliding velocity of ith pad
R_1 = radius from c.g. to upper leg hardpoint (Fig. 5)
R_2 = radius from c.g. to lower leg hardpoint (Fig. 5)
t = time
V_v, V_h = vertical and horizontal velocity of vehicle (gravitational axes)
x,y,z = coordinates of center of gravity of vehicle (Fig. 6)
x_{pi}, y_{pi}, z_{pi} = coordinates of the ith pad (Fig. 6)
α = ratio of full-scale acceleration to model acceleration
β = ratio of full-scale mass to model mass
γ = ratio of full-scale length to model length
α_j = angle between upper and lower gear hardpoints (Fig. 5, note sign convention)
Δ_p = horizontal distance from leg set joint to lower surface of landing pad (Fig. 6)
ζ = slope of surface (Fig. 6)
θ = angle moved through by model from point of release to point of ground contact (Fig. 3)
θ_i = angle of a particular leg set (Fig. 5)
μ_i = coefficient of friction of ith pad with lunar surface
σ_p = crush strength of crushable pad
ψ = angular rotation of vehicle about z axis (pitch) (Fig. 6)
ψ_0 = initial pitch angle

Subscripts

i = denoting association with ith leg set (i = 1,2, ... n)
j = denoting association with jth shock strut (j = 1,2,3)

Introduction

THE design of a lightweight landing gear system for a spacecraft depends upon anticipated impact conditions, such as horizontal and vertical velocities, vehicle orientation, ground slope limitations, and surface conditions. For a manned, soft landing on the moon, studies indicate that a leg-type landing gear is probably best.[1, 2] Each leg consists of an inverted-tripod arrangement (Fig. 1) of three stroking struts which contain crushable, energy-absorbing material. The upper strut constitutes the main energy absorber of the system. The high efficiency of this structure is because it is primarily axially loaded. Transverse loads are limited to those generated by end point lateral decelerations and nonsymmetrical loading of the landing pad that introduces only slight bending moments into one of the lower struts. Both deceleration of the end points and the magnitude of bending moments from nonsymmetrical ground forces can be limited by constructing the landing pad of crushable material. Several research groups have more or less independently arrived at this type of landing gear system in which each leg is an inverted tripod.

The present paper is concerned with an experimental and theoretical study of the tripodal gear system. The study may be divided into three areas: 1) experimental drop tests of a dynamically scaled model, 2) development of a theoretical model that correlates with the experimental results, and 3) parametric studies using the theoretical model.

Model Scaling

The design of a scale model of a spacecraft for purposes of landing gear system evaluation makes use of the standard methods of dimensional analysis.[3] Each of the basic vehicle

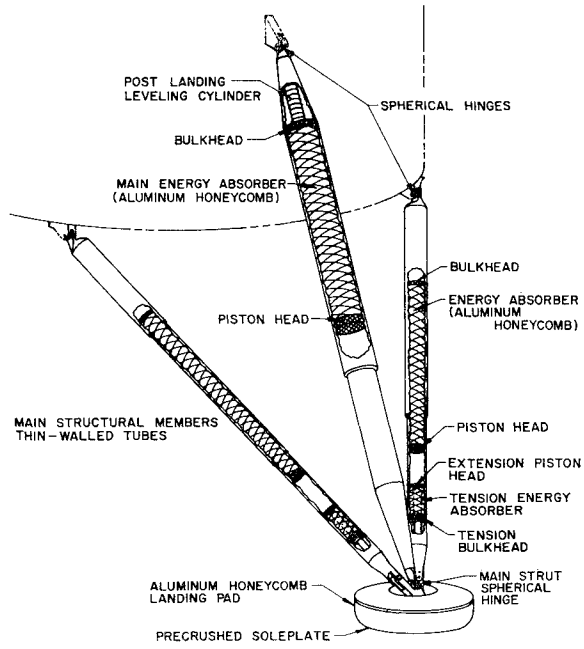

Fig. 1 Inverted tripod leg with universal energy absorption characteristics.

and gear parameters can be expressed by various combinations of the three-dimensional units of force, length, and time, which can, in turn, be expressed in units of acceleration, length, and mass. Three scale factors, α, β, and γ, are defined in the Nomenclature.

If all of the terms within one of the π quantities characterizing a particular problem are scaled by these factors, then the resulting quantity for the model π_1 will be identical to the full-scale quantity π_2. For example, one of the π quantities is

$$\pi = m\,gR_1/I\dot{\psi}_0^2 \tag{1}$$

By employment of the scaling factors, the requirement that $\pi_1/\pi_2 = 1$ is reduced to the identity

$$\left(\frac{1}{\beta}\right)\left(\frac{1}{\alpha}\right)\left(\frac{1}{\gamma}\right)(\beta\gamma^2)\left(\frac{\alpha}{\gamma}\right) = 1 \tag{2}$$

The scale factor α is fixed at the ratio of lunar or planetary gravitational acceleration to earth gravitational acceleration. Any attempt to change this factor would involve a complex drop test scheme, such as dropping the model on an accelerating platform or compensating for gravity by a gymballed thrustor at the center of gravity of the model. The other two factors, β and γ, depend upon the information desired from the model tests. For stress information, the model should be made of the same material as the full-scale system and should be subjected to the same stress. For a lunar model, this would mean

$$\alpha = \tfrac{1}{6} \qquad \beta/\gamma^3 = 1 \qquad \alpha\beta/\gamma^2 = 1 \tag{3}$$

hence, $\beta = 6^3$ and $\gamma = 6$.

If, however, one desires only to predict the motion of the vehicle, then stress by itself need not be scaled. This leaves considerable latitude on the selection of β and γ, but there are practical limitations. If γ is very large, then the model legs can not be scaled, because of a practical minimum on strut wall thickness. This, in turn, results in difficulty in obtaining the correct moment of inertia of the model, since considerable mass is located at a large distance from the center of gravity. Decreasing β would tend to alleviate this, except that it results in an increase in model-gear stroke force which necessitates increasing the strut cross sections

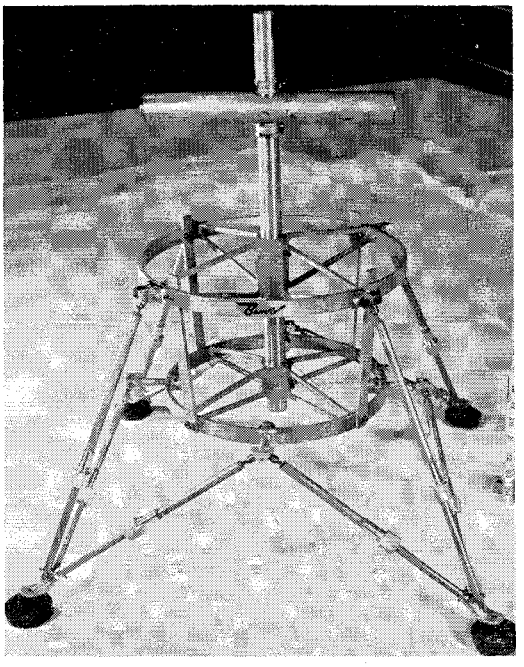

Fig. 2 Dynamically scaled model of 300 slug vehicle; $\gamma = 10$.

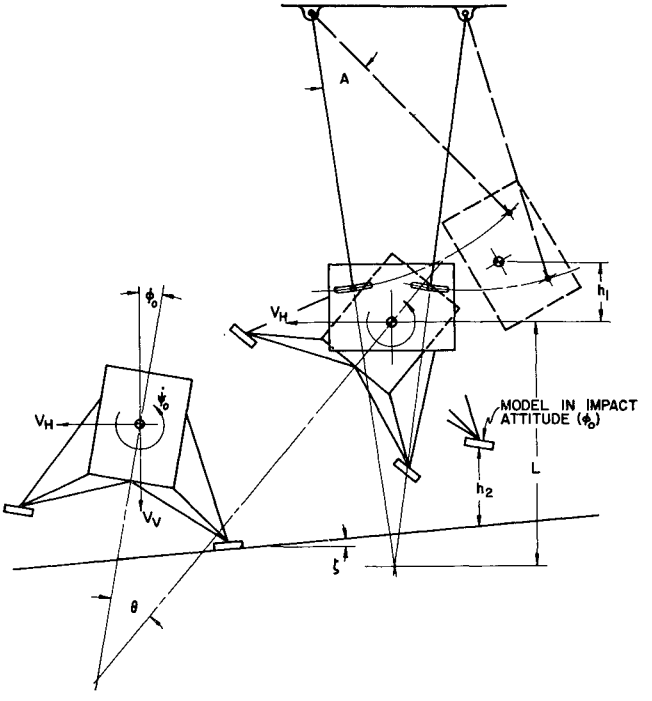

Fig. 3 Schematic of drop test mechanism.

and, therefore, mass. For these reasons, the stress scaled model given by Eq. (3) is a good starting point. Material limitations indicate that deviations from this "ideal model" by a vector of $3(\gamma \simeq 20)$ are approaching the maximum for a model that is to be dynamically scaled for over-all vehicle motion. Once values of α, β, and γ are chosen, derived scaling factors may be determined for other quantities as shown in Table 1.

Models and Drop Test Equipment

Two models are considered. The first simulates a comparatively large vehicle with an over-all height (including the landing gear system) of 70 ft and a lunar touchdown mass of 2000 slugs. A length scaling factor of $\gamma = 20$ provides a convenient model size. (See parameters in Table 1 under $\gamma = 20$.) In the full-scale system, each of the stroking struts would contain crushable aluminum honeycomb energy absorbers. On the model, stroking loads were more conveniently achieved by using the sliding friction of a tapered Teflon sleeve compressed against the shock-strut piston by an adjustable collar threaded to the outer diameter of the sleeve. (Teflon is suitable because the ratio between static and dynamic coefficients of friction is close to unity.) Periodic adjustment of the friction devices assured a relatively consistent load. The second model (Fig. 2) considered simulates a vehicle with an over-all height of 18 ft (including landing gear system) and a lunar touchdown mass of 300 slugs; the length scaling factor is $\gamma = 10$. Again, the energy absorber in each of the struts is simulated by a friction sleeve.

Both models have four legs because analog computer studies had indicated that, for equal stability and energy absorption capability, the four-legged vehicles should be the lightest. (Although the analog model was based on legs with unidirectional stroke, in contrast to the actual triaxial stroke capability of a tripodal leg, a more detailed analysis to be discussed later confirmed this four-leg conclusion.)

The drop test mechanism, a four-link pendulum (Fig. 3), is designed to allow for any combination of horizontal and vertical velocities, pitch angle (ψ_0), and pitch velocity ($\dot{\psi}_0$) at the instant of impact. This was achieved by making the angle between the two vertical links of the pendulum adjustable. The model was attached to the lower horizontal link, so that the model's c.g. coincided with the c.g. of the link. This lower link is the only significant moving mass in the pendulum. The whole system is rotated backward to raise the center of gravity an amount h_1; then it is released. At the instant that the velocity vector of the lower link and model is horizontal, the horizontal velocity and the pitch velocity are given by

$$V_H{}^2 = \frac{2gh_1(m_0 + m)L^2}{(m_0 + m)L^2 + (I_0 + I)} \tag{4}$$

and

$$\dot{\psi}_0 = V_H/L \tag{5}$$

Table 1 Derived scale factors

Quantity	Scale factor (f = full scale, m = model	$\gamma = 20$ ($\alpha = \frac{1}{6}$, $\beta = 20^3$)	$\gamma = 10$ ($\alpha = \frac{1}{6}$, $\beta = 10^3$)	$\gamma = 6$ ($\alpha = \frac{1}{6}$, $\beta = 6^3$)
Angular velocity	$\dot{\theta}_f/\dot{\theta}_m = (\alpha/\gamma)^{1/2}$	0.0915	0.129	0.167
Energy	$W_f/W_m = \alpha\beta\gamma$	2.67×10^4	1.67×10^3	2.16×10^2
Force	$F_f/F_m = \alpha\beta$	1.333×10^3	1.67×10^2	36.00
Mass density	$\rho_f/\rho_m = \beta/\gamma^3$	1.00	1.00	1.00
Mass moment of inertia	$I_f/I_m = \beta\gamma^2$	3.2×10^6	1×10^5	7.776×10^3
Pressure, stress, etc.	$E_f/E_m = \alpha\beta/\gamma^2$	3.33	1.67	1.0
Spring rate	$K_f/K_m = \alpha\beta/\gamma$	66.7	16.7	6.0
Time	$t_f/t_m = (\gamma/\alpha)^{1/2}$	10.93	7.75	6.0
Velocity	$V_f/V_m = (\alpha\gamma)^{1/2}$	1.823	1.291	1.0

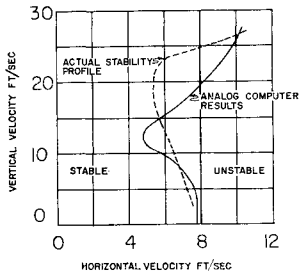

Fig. 4 Comparison between actual stability profile and theoretical profile using simplified mathematical model.

At this point the model is released automatically by a mechanism controlled by a microswitch. The model c.g. follows a parabolic trajectory to the surface simulator, and the model moves through a pitch angle

$$\theta = \dot{\psi}_0 V_v/g \tag{6}$$

This requires a correction angle on the model's pitch angle in the rotatable release platform. The drop height h_2 is measured between the surface and the impacting pad, with the model located on the release platform with the uncorrected pitch angle (impact pitch angle). Although this distance is not the actual drop height, the vertical velocity achieved at impact is related to it by the relationship

$$h_2 = V_v(V_v - V_H \tan\zeta)/2g \tag{7}$$

To facilitate the testing, charts were developed for the settings on platform angle, link setting, drop height (h_b), and release angle necessary to achieve at impact any desired combination of velocities and orientation.

Mathematical Model of System

Preliminary investigations had been made with a mathematical model in which each leg had only unidirectional stroke. An attempt was made to account for some nonunidirectional effect by varying the coefficient of friction between the ground and the pad, but the variation in vertical and horizontal loads, and stabilizing and destabilizing moments generated by these loads, is so complex that it is impossible to represent the effect by equating the horizontal load to a vertical load multiplied by a coefficient of friction.

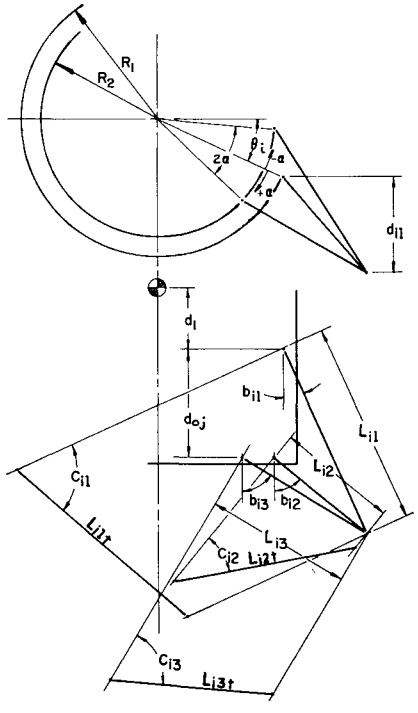

Fig. 5 Tripodal leg-system nomenclature.

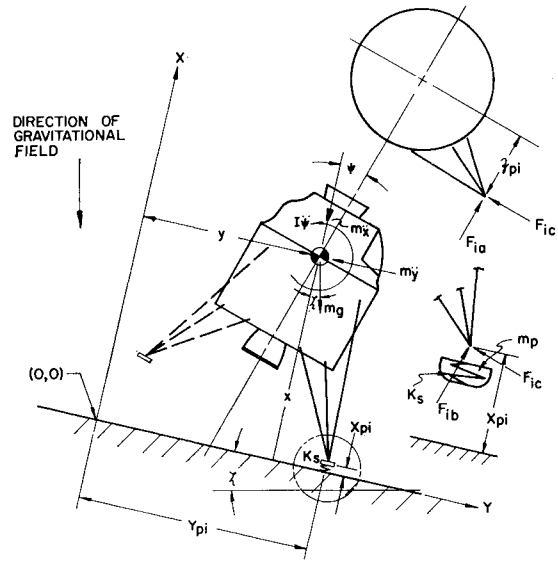

Fig. 6 Vehicle free-body diagram and nomenclature.

Figure 4 shows the poor degree of correlation achieved with such a mathematical model, because of the interplay between geometry changes and load changes and the fact that the tripodal gear results in triaxial energy absorption. It was concluded that the complete articulation and stroke capabilities of the landing gear system must be duplicated to yield a true picture of vehicle stability during landing.

Nomenclature used in the analytical model is given in Figs. 5, 6, and 7. Figure 7 shows the nomenclature associated with the stroking load F_{ij}. For the studies conducted, a constant stroking force (F_j) was assumed for the crushable honeycomb absorber. The derivation of the nonlinear equations of motion for the vehicle is straightforward. The equations governing the system are listed below.

Geometry

Let

$$A = L_{i1}\sin b_{i1} + R_1\cos\theta_i - R_j\cos(\theta_i + \alpha_j) \tag{8}$$

$$B = L_{i1}\cos b_{i1} - d_{0j} \tag{9}$$

$$C = d_{i1} + R_1\sin\theta_i - R_j\sin(\theta_i + \alpha_j) \tag{10}$$

Then the leg set geometrical relationships are:

$$L_{ij}^2 = A^2 + B^2 \tag{11}$$

$$L_{ijt}^2 = L_{ij}^2 + C^2 \tag{12}$$

$$b_{ij} = \tan^{-1}A/B \tag{13}$$

$$c_{ij} = \tan^{-1}L_{i1}/C \tag{14}$$

The pad coordinates are given by

$$x_{pi} = x - d_1\cos\psi - R_1\cos\theta_i\sin\psi - L_{i1}\cos(b_{i1} - \psi) \tag{15}$$

$$y_{pi} = y - d_1\sin\psi + R_1\cos\theta_i\cos\psi + L_{i1}\sin(b_{i1} - \psi) \tag{16}$$

$$z_{pi} = d_{i1} + R_1\sin\theta_i \tag{17}$$

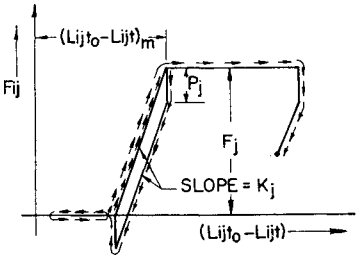

Fig. 7 Energy absorber nomenclature.

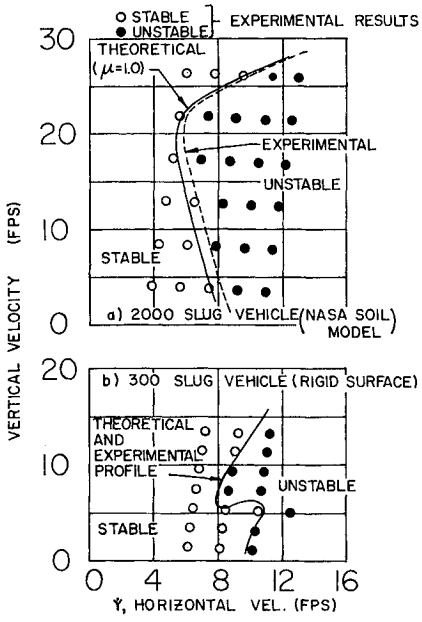

Fig. 8 Comparison of theoretical and experimental profiles.

Forces

Let

$$\Delta L = L_{ijt0} - L_{ijt} \tag{18}$$

$$\Delta L_M = \text{maximum previous value of } \Delta L \tag{19}$$

Then the stroke force is given by

$$\begin{aligned} F_{ij} &= K_j[\Delta L - \Delta L_M + F_j/K_j], \\ &\quad \Delta L_M - F_j/K_j < \Delta L < \Delta L_M,\ (d\Delta L/dt) > 0 \\ &= K_j[\Delta L - \Delta L_M + F_j/K_j] - P_j, \\ &\quad \Delta L_M - F_j/K_j < \Delta L < \Delta L_M,\ (d\Delta L/dt) < 0 \\ &= F_j, -\Delta L_M < \Delta L \\ &= 0, -0 < \Delta L < \Delta L_M - F_j/K_j \\ &= K_{Ej}\Delta L, -\Delta L < 0 \end{aligned} \tag{20}$$

The ground reaction force is

$$\begin{aligned} F_{ix} &= K_s(\Delta p - x_{pi}) \qquad x_{pi} \leq \Delta p \\ &= 0 \qquad\qquad\quad x_{pi} > \Delta p \end{aligned} \tag{21}$$

Resolution of the stroke forces into the vehicles axes system gives

$$F_{ia} = \sum_j F_{ij} \operatorname{cosc}_{ij} \tag{22}$$

$$F_{ib} = \sum_j F_{ij} \operatorname{sinc}_{ij} \operatorname{cosb}_{ij} \tag{23}$$

$$F_{ic} = \sum_j F_{ij} \operatorname{sinc}_{ij} \operatorname{sinb}_{ij} \tag{24}$$

Equations of Motion

The equations of motion of the vehicle are

$$m\ddot{x} - mg\cos\zeta = \Sigma_i (F_{ib}\cos\psi + F_{ic}\sin\psi) \tag{25}$$

$$m\ddot{y} - mg\sin\zeta = \Sigma_{ib} (F_{ib}\sin\psi - F_{ic}\cos\psi) \tag{26}$$

$$I\ddot{\psi} = \textstyle\sum_i [F_{ic}(d_1 + L_{i1}\cos b_{i1}) - F_{ib}(R_1\cos\theta_i + L_{i1}\sin b_{i1})] \tag{27}$$

The equations of motion of the unsprung mass are

$$m_p\,\ddot{x}_{pi} + F_{ib}\cos\psi + F_{ic}\sin\psi - F_{ix} = 0 \tag{28}$$

$$m_p\,\ddot{y}_{pi} - (F_{ic}\cos\psi - F_{ib}\sin\psi) + \mu_i F_{ix}\dot{y}_{pi}/\dot{s}_i = 0 \tag{29}$$

$$m_p\,\ddot{z}_{pi} - F_{ia} + \mu_i F_{ix}\dot{z}_{pi}/\dot{s}_i = 0 \tag{30}$$

where

$$\dot{s}_i = (\dot{y}_{pi}^2 + \dot{z}_{pi}^2)^{1/2} \tag{31}$$

The dynamics of the unsprung mass of each leg have been included in the equations of motion to allow the determination of footpad motion. The numerical value of the unsprung mass in these equations does not have to equal the true unsprung mass of the legs in order to obtain correct vehicle and gear motions during landing, but it can not be so high that it constitutes a significant percentage of the over-all mass of the vehicle. If predictions of unsprung mass accelerations are desired, then, of course, the numerical value must equal the actual unsprung mass. Such calculations would require a smaller time increment in the numerical solution than a solution using a larger mass value due to the high-frequency "loop" made up of the unsprung mass and the elastic portion of the strut load-stroke curves.

Comparison of Experimental and Theoretical Results

For the $\frac{1}{20}$-scale model of the 2000-slug vehicle, the critical boundary between stable and unstable landing as a function of vertical and horizontal velocities was established for a back-pitched, zero-pitch-velocity landing condition. The landings took place on a 5° surface with the gears oriented to yield the minimum stabilizing moment (2-2 impact of the 4 legs). The surface itself was a scaled version of a soil model suggested by NASA[4]: the upper layer was $\frac{1}{4}$ in. of fine pumice stone powder, simulating a 10-cm layer of igneous rock dust; below this, 2 layers of foamed plastics simulated substrata of rock froth. However, the analytical model assumed a rigid impact surface with a coefficient of friction of unity. A comparison between the theoretical and experimental results for this case is shown in Fig. 8a.

Tests conducted with the $\frac{1}{10}$-scale model of the 300-slug lunar vehicle (Fig. 8b) were carried out using a rigid surface (plywood) rather than the scaled lunar surface just described. A very high coefficient of friction was obtained between the surface and the landing pads by attaching sharp barbs to the pads to simulate landing on a very rocky surface. The landing conditions again were a downhill 2-2 back-pitched impact on a 5° slope.

For both models, the correlation between theory and experiment is satisfactory. The study also indicates that, for

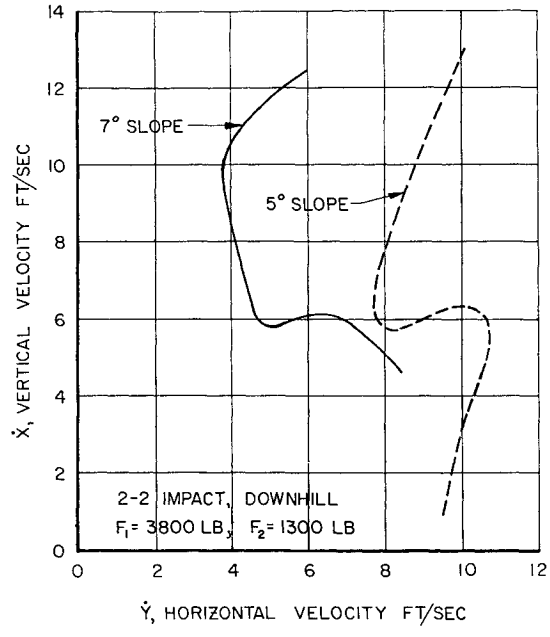

Fig. 9 Effect of ground slope on stability boundaries.

the size of vehicles under consideration, the energy losses and "dust flow" forces generated when the pads contact the lunar dust are not of sufficient magnitude to affect stability and over-all motion. The assumption of a rigid surface appears to be valid for the suggested soil model, in which the first substrata of rock froth was assumed to have a bearing strength of 200 psi. This would support the particular landing pad and would be equivalent to a rigid surface. The design of a landing pad for any particular surface bearing pressure is governed by the following equation:

$$A_p = 1/\sigma_p(F_c + m_p V_v^2/2L_p) \qquad (32)$$

Nonpenetration of the surface would require that σ_p be less than the bearing strength of the surface.

The assumption that the unsprung mass of the gears (and the associated dynamics) does not affect the over-all vehicle motion appears to be valid. It is generally concluded that the analytical model is sufficiently detailed to predict vehicle and landing gear action during landing.

Parametric Studies

The failure modes of the landing gear system could be categorized as follows:

1) Excessive horizontal or vertical forces transmitted to the vehicle
2) Final attitude too far from vertical (or vehicle topples)
3) Energy capacity of any shock strut exceeded
4) Strut crushes against vehicle frame because of excessive stroke
5) Ground clearance for nozzle falls short of specified minimum
6) Structural failure of any strut occurs

No failure item from the failure mode list can be picked as the sole criterion for the evaluation of the landing gear system. For example, one of the most critical of these items is the over-all vehicle stability, but design for stability alone leads to bottoming of the auxiliary struts on a one-leg-forward, uphill impact at maximum horizontal and vertical velocities.

For the 300-slug vehicle, the spectrum of landing conditions considered is as follows:

1) Vertical descent velocity, 0 to +10 fps
2) Horizontal velocity, −5 to +5 fps
3) Pitch or yaw angular velocity, −0.10 to +0.10 rad/sec
4) Roll velocity, 0

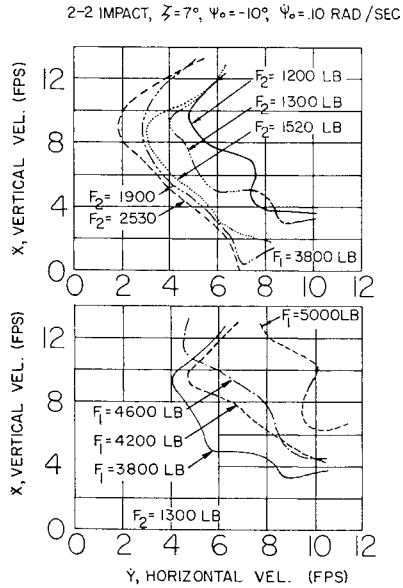

Fig. 10 Effects of lower (F_2) and upper (F_1) strut stroke loads.

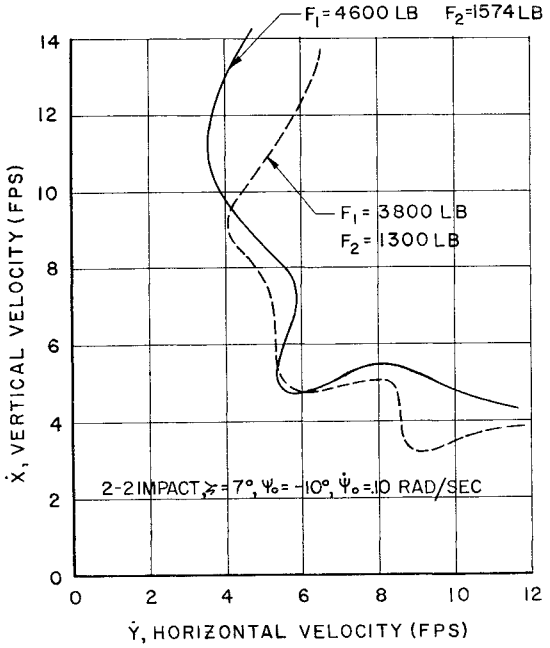

Fig. 11 Effect of variation in stroke load for $F_1/F_2 = 2.92$.

5) Pitch or yaw angle (with respect to gravitational field), −5° to +5°
6) Roll angle, no limits (landing in any direction)
7) Ground slope, 0° to 5°
8) Surface coefficient of friction, 0 to ∞
9) Maximum ground roughness height, 4 in.

The vehicle was assumed to be cylindrical with a radius of 6 ft, a nozzle-to-c.g. height of 8.5 ft and a radius of gyration of 4.5 ft. It was found that a landing gear system having a radius of 10 ft, an upper strut stroke load of 3800 lb, and a lower strut stroke load of 1300 lb, both satisfied the critical combinations of the impact variables without failure and was near-optimum from a weight standpoint. The upper gear hardpoint was located 1.5 ft below the c.g., and the lower gear hardpoint was approximately 5 ft below this. Both of the hardpoints were considered as fixed in the weight optimization study.

The "null point" landing gear system used for most of the parameter variation studies discussed below consisted basically of the forementioned system with the exception that the gear radius was increased to 12 ft.

One of the first items considered was ground slope. Compounding a 4-in. ground ledge, a 4-in. ground depression, and a 5° slope results in an effective slope of approximately 7° for the gear radius of 12 ft. Figure 9 shows that ground slope has a marked effect on vehicle stability; the increase from 5°–7° results in a 50% reduction in the allowable maximum horizontal velocity at impact.

Ground slope capability, of course, can be increased by increasing the radius of the landing gear. For the forementioned spectrum of landing conditions, the radius requirements for 5° and 7° slopes are 10 and 12 ft, respectively, and it will be shown later that $dR/d\zeta$ is nearly constant for $5° < \zeta < 20°$.

The energy-absorbing lower struts, necessary to keep the horizontal acceleration of the vehicle low, also enhance the stability of the vehicle when the line of action of the lower struts falls below the c.g. of the vehicle. (If the lower gears were only elastically compressible, extremely high overturning moments could be generated when the forward leg contacted a horizontal obstruction; the only stabilizing influence would be the gravitational force). Figure 10 (top) shows that decreasing the lower strut stroke load F_2 (with fixed upper strut stroke load F_1) has a stabilizing effect, i.e.,

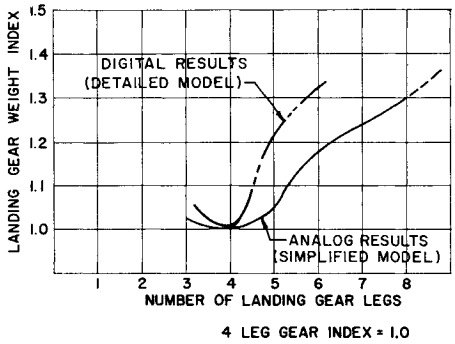

Fig. 12 Weight vs number of landing gear leg sets, equal stability, and equal absorption capability.

it permits greater horizontal velocities. However, the permissible reduction in F_2 is established by the critical energy absorption impact. For an uphill impact at maximum vertical and horizontal velocities and with the vehicle pitch toward the slope, drop tests as well as computer studies indicate that the forward leg set (1-2-1 leg orientation) absorbs a high percentage of the total kinetic energy of the system. For the present system, this percentage is 72%, 32% of which is absorbed by the lower struts. Thus with too low an F_2, the stroke becomes excessive and failure can occur by either lower strut bottoming or structural interference of the upper strut with the lower edge of the vehicle body.

An increase in the upper or main strut stroke load F_1 (with fixed F_2) is stabilizing (Fig. 10, bottom). This would be expected on the basis of the previous discussion because the line of action of the upper struts falls above the c.g. of the vehicle so that an increase in the ratio between stabilizing and destabilizing moments results. Figure 11 shows that when the ratio F_1/F_2 is held constant, there is very little change in the stability.

Although an increase in F_1 increases the maximum allowable horizontal velocity, it leads to added weight and to increases in the horizontal and vertical decelerations during impact. The weight increase can be partially compensated by reducing the radius, but this shortens the lower struts and requires a greater lower strut stroke load to take care of the critical one-leg energy condition. Tradeoffs among these factors lead to an F_1 of approximately 4600 lb to take care of the stability on a 7° slope for the specified velocity spectrum.

The optimum number of legs for a system can not be established without defining ground rules. For example, on the surface it would appear that over-all landing reliability could be increased by increasing n, the number of leg sets, because with $n > 4$, failure of one leg set would not necessarily result in a toppling failure.

However, it can be shown that for two systems of n and $n + 1$ legs, respectively ($n \geq 4$), the increased probability of failure brought about by the greater number of parts in the $n + 1$ system overshadows the gain in reliability achieved by generation of a small region of one-leg-failed stability. The selection of the optimum number of leg sets, therefore, depends primarily on weight considerations. Conceivably, the use of a large number of legs could lead to a reduction in the required size of each leg and a weight advantage.

Analog computer studies of landing gear systems, designed for equal stability with equal energy-absorption characteristics with unidirectional-stroke shock struts, indicated that, in fact, a four-leg system was the lightest. Later studies using the more detailed digital-computer model verified this conclusion (Fig. 12). The latter studies showed that a 5-leg system would be 25% heavier than the equivalent 4-leg system, because the gear radius of a 5-leg system had to be the same as that of a 4-leg system, and the critical energy landing requirements were the same for both systems—$\frac{3}{4}$ of the total vehicle kinetic energy had to be absorbed on one leg with $\frac{1}{3}$ of this energy being absorbed by the lower struts. Thus, there could be no reduction in F_2 for the 5-leg system without incurring a lower-strut bottoming failure. The stability profiles showed slight differences similar to those of Fig. 11. This could be expected since the higher stroke loads of the solid line of Fig. 11 would be analogous to the 25% higher over-all loads found in the 5-leg system.

A wide-track (Fig. 13) design for ground slopes up to 15° was investigated using the mathematical model given previously. The gear size was limited by the gear stowage space which, in turn, was determined by the clearance between the booster adapter fairing and the landing vehicle under consideration. In contrast to the system designed for a 7° slope, the line of action of the lower struts passes above the c.g. of the vehicle. This factor, combined with the smaller angle

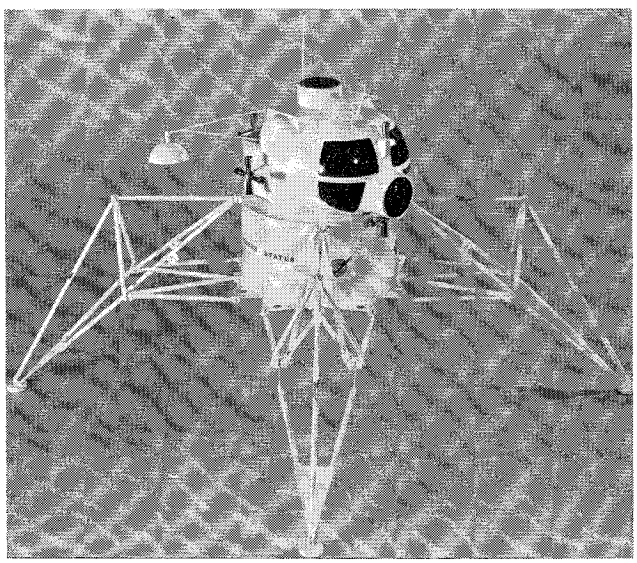

Fig. 13 Wide-track landing gear system.

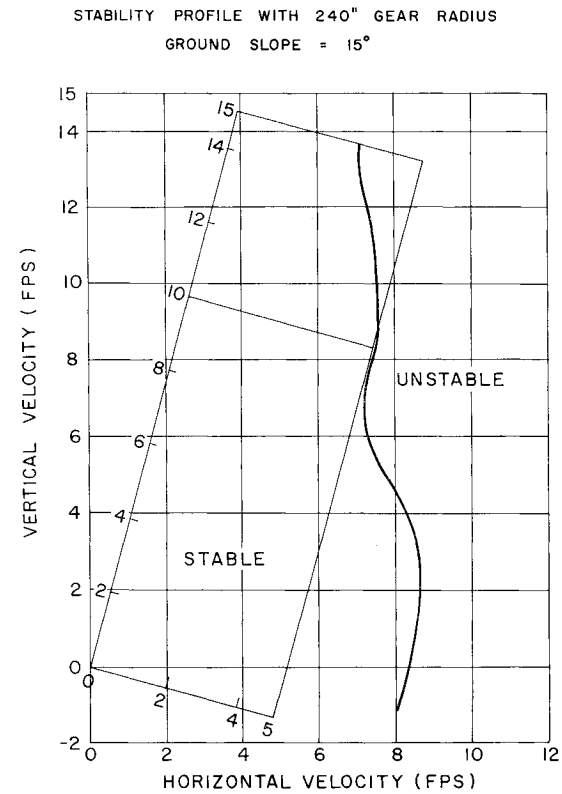

Fig. 14 Stability profile for wide-track system on 15° slope.

between the two lower struts of a leg set, resulted in some marked differences in performance trends. Reduction of F_2 had a destabilizing influence because very large strokes were encountered in the outside lower strut of the forward leg sets for the critical 2-2 downhill impact condition. In fact, with the first design of the wide-track system, the forward leg sets had a tendency to act as a single spherically hinged strut. Increasing the angle between the lower legs, reducing F_1 and increasing F_2 alleviated this problem. Figure 14 shows the over-all stability profile. The inclined coordinates are velocities relative to the gravitational field, whereas the main coordinates are measured with respect to the (sloped) surface. It can be seen that the system is stable for the given spectrum of velocities.

General Trends and Conclusions

In all of the gear designs discussed previously, the critical landing conditions are fairly consistent. The maximum vertical deceleration occurs on a straight drop onto a level surface of high coefficient of friction for which case all legs stroke together. Maximum horizontal deceleration occurs during a nearly horizontal drop onto a surface of high coefficient of friction (simultaneous obstacle impact of all leg sets), but the deceleration quickly drops off due to pitching of the vehicle.

The landing that is critical from a stability standpoint is a downhill, back-pitched impact with the minimum stabilizing radius on the forward leg sets (i.e., a 2-2 impact for a four-leg system), because it results in a high forward pitch velocity that must be decelerated by the forward legs. Landing in a forward-pitched attitude is more stable, since the impact reaction moment now simply rights the vehicle.

The critical energy-absorption landing condition consists of an uphill, one-leg-forward impact with forward pitch velocity on an infinite coefficient of friction surface (for the forward leg set). This landing condition is particularly critical for systems having a low ratio of gear radius to c.g. height. With higher values of the latter ratio, the high moment generated by the forward leg causes the vehicle to pitch rearward more rapidly, thus bringing the other legs into play with a more uniform energy distribution. For sufficiently high ratios of radius to c.g. height, the critical stability condition becomes the critical stroke condition for the lower legs, due to the back-swiveling of the forward legs as previously described.

The critical post-landing attitude, for both high and low values of the radius/c.g.-height ratio, occurs on uphill landing with an infinite coefficient of friction on the forward leg or legs, and a zero coefficient on the aft leg. For the small-radius, 7° design, the most adverse post-landing attitude

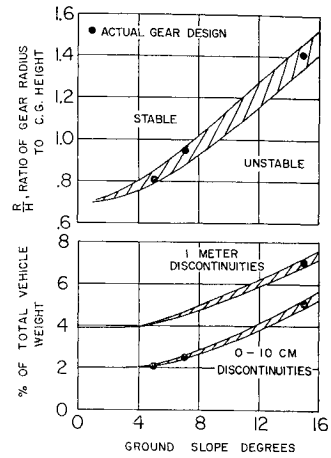

Fig. 15 Radius and gear weight trends as a function of ground slope.

was 18° (from gravitational vertical), but for the wide-track design landing on a 15° slope, the adverse post-landing attitude was again 18°, or only 3° more than the ground slope.

The generalizations already given concerning effects of stroking loads cover parameter variation trends about two widely separated null points of design. Both the stroking loads and the stroke-load ratios play a very important part in the stability of the vehicle.

The general trends in weight and radius/c.g.-height ratio found in the three landing gear designs are shown in Fig. 15. The system designed for ground slopes up to 15° also included capability of landing on surfaces with discontinuities as high as 1 meter. This required considerable shielding around the lower struts in the form of crushable material and also necessitated designing these lower struts for large bending moments brought on by the discontinuity impact, so that landing gear weight was nearly doubled. Subtracting this weight penalty for large discontinuities yielded the point shown in the lower weight curve of Fig. 15. It is emphasized that the points shown in this figure represent complete designs taking into account all of the design criteria.

References

[1] Duke, W., "Lunar landing problems," *Advances in the Astronautical Sciences* (American Astronautical Society, New York, 1963), Vol. 10, pp. 102–155.

[2] "Lunar landing module alighting gear," Bendix Rept. MM-62-2 (870, 858-1) (March 1962), unpublished.

[3] Langhaar, H. L., *Dimensional Analysis and Theory of Models* (John Wiley and Sons, New York, 1951), Chaps. 2 and 3, 13–43.

[4] Kovit, B., "LEM: Our first true spacecraft," *Space/Aeronautics* (Conover-Mast Publications Inc., New York, March 1963) p. 82.